

INITIAL RESULTS OF A MODEL ROTOR HIGHER HARMONIC CONTROL (HHC)  
WIND TUNNEL EXPERIMENT ON BVI IMPULSIVE NOISE REDUCTION

BY

W.R. SPLETTSTOESSER, G. LEHMANN, B. VAN DER WALL

GERMAN AEROSPACE RESEARCH ESTABLISHMENT (DLR)  
BRAUNSCHWEIG, WEST-GERMANY

**FIFTEENTH EUROPEAN ROTORCRAFT FORUM**

SEPTEMBER 12 - 15, 1989 AMSTERDAM

INITIAL RESULTS OF A MODEL ROTOR HIGHER HARMONIC CONTROL (HHC)  
WIND TUNNEL EXPERIMENT ON BVI IMPULSIVE NOISE REDUCTION

by

W.R. SPLETTSTOESSER, G. LEHMANN, B. VAN DER WALL,  
GERMAN AEROSPACE RESEARCH ESTABLISHMENT (DLR)  
BRAUNSCHWEIG, WEST-GERMANY

Summary

Initial acoustic results are presented from a higher harmonic control (HHC) wind tunnel pilot experiment on helicopter rotor blade-vortex interaction (BVI) impulsive noise reduction, making use of the DFVLR 40%-scaled BO-105 research rotor in the DNW 6m by 8m closed test section. Considerable noise reduction (of several decibels) has been measured for particular HHC control settings however, at the cost of increased vibration levels and vice versa. The apparently adverse results for noise and vibration reduction by HHC are explained. At optimum pitch control settings for BVI noise reduction, rotor simulation results demonstrate that blade loading at the outer tip region is decreased, vortex strength and blade vortex miss-distance are increased, altogether resulting in reduced BVI noise generation. At optimum pitch control settings for vibration reduction adverse effects on blade loading, vortex strength and blade vortex miss-distance are found. Further investigations into validation and optimization of the HHC potential for rotor noise and vibration reduction is recommended.

1 Introduction

Helicopter rotor blade-vortex interaction (BVI) impulsive noise has in recent years become the subject of intensive research. When BVI occurs, this noise mechanism dominates the noise radiation in the frequency range most sensitive to human subjective response. The impulsive noise due to BVI originates from the unsteady aerodynamic interaction of a lifting and translating rotor blade with the trailing vortex system generated by preceding blades. This phenomenon is predominantly observed during descent and manoeuvre flight condition when the miss-distance of the rolled-up tip vortices and the rotor plane becomes extremely small.

Past experimental work on rotor BVI noise was performed to define the rotor operating regimes for BVI [1-4], the primary parameters affecting BVI noise generation [e.g. 5-8], and the scaling conditions of the BVI acoustic signals for model-scale testing [6,7]. The directivity pattern of advancing and retreating side BVI was determined in [9], and the acoustic source locations in the rotor plane were identified [4,10,11,12], indicating that the acoustically active sources are concentrated in the first and fourth quadrant on relatively small areas, where blade and vortex axes are close to parallel.

Semi-empirical methods making use of the acoustic analogy formulation [13-15] and of measured unsteady absolute blade pressures allowed to calculate the BVI acoustic waveforms of a scaled model rotor [16-19]. The dipole-type source term, one of the three source terms of the Ffowcs Williams-Hawkings equation most important for BVI noise, requires the absolute blade surface pressures (steady and unsteady components) as input, indica-

ting the strong correlation of the BVI impulsive noise generation with both, the steady and unsteady blade loading. Combining these findings and the knowledge of the exact BVI source locations in the rotor plane as shown in |12| the idea was discussed and subsequently realized to apply the higher harmonic control (HHC) technique to the BVI impulsive noise reduction problem. This active pitch control concept for vibration reduction, recently developed by the DFVLR Institute for Flight Mechanics for the BO-105 model rotor |20-22|, allows control of the blade angle of attack and thus its lift (loading) at any radial and azimuthal location in the rotor plane.

The potential benefit of the HHC concept for BVI noise reduction was recently suggested in |23|. Based upon analysis of a simplified, two dimensional physical model, the critical parameters controlling BVI noise generation were identified. Primary parameters were shown to be vortex strength and local blade lift, both proportional to the sound generation, and the blade-vortex separation distance with inverse square correlation, which agree well with the findings of other researchers |e.g. 24|. Efforts of increasing the vortex core size (in order to decrease the induced velocity distribution) by tip shape variations, guide vanes and porous tips, or of enforcing the vortex dissipation by winglets have shown only minor reductions of BVI noise generation |25, 26|.

All of the three dominant parameters might be manipulated by HHC for noise control, however that is not an easy task to do and until now there are no results available in the public domain. Therefore, the major objective of the present work was to investigate the possible effect of HHC on these primary parameters and the related BVI noise radiation, and simultaneously on rotor vibration, without reducing the overall performance. The test was performed as a hook-up experiment of preliminary character during a major HHC demonstration campaign in the DNW in March 1988.

## 2 HHC Concept and Application for BVI Noise Reduction

The original objective for the development and the application of HHC is the improvement of helicopter ride quality. The motivation is based on the very high vibration levels of a helicopter compared with those of a fixed wing aircraft which represent a considerable stress for material and crew. There are several physical phenomena contributing to the vibration levels in cruising flight and especially in extrem flight conditions, e.g.

- the velocity distribution of the rotor inflow and
- impulsive flow due to blade-vortex interaction at low and moderate speed

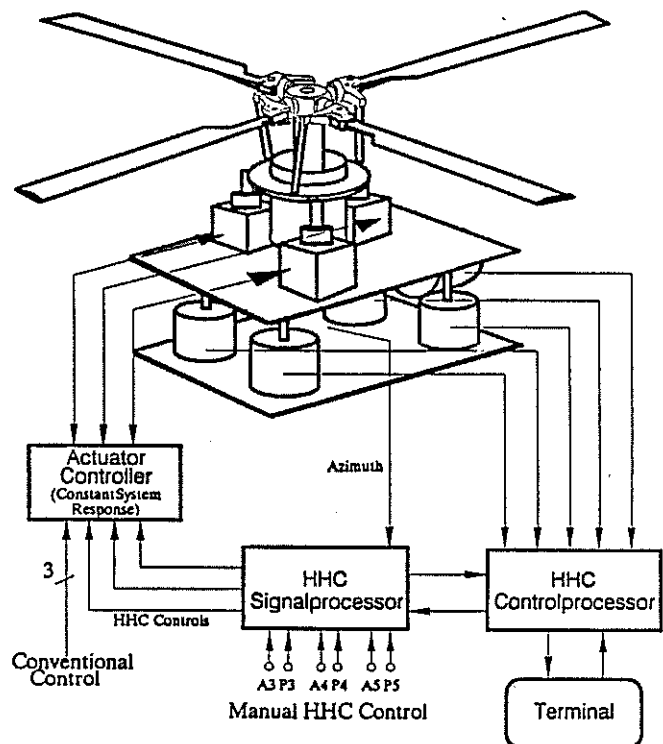


Fig. 1 Schematic of Higher Harmonic pitch Control (HHC) hardware

- stalled and reversed flow on the retreating blade at high speed

The helicopter rotor mainly responds at harmonics of the blade passage frequency  $\Omega_{BP} = nb\Omega_R$ , where  $n$  is the number of the harmonic,  $b$  the number of blades and  $\Omega_R$  the frequency of rotation. But due to the kinematical transformation from a rotating system (rotor) to a fixed frame (fuselage) the  $(nb-1)$  and  $(nb+1)$  harmonic blade loads are also contributing to the  $(nb\Omega_R)$  harmonic vibrations.

The basic idea of HHC is to reject these harmonic disturbances by modifying the blade root pitch with the same frequencies. In the case of a four-bladed rotor the option exists to control at 3-, 4-, or 5-per-revolution in addition to the conventional 1-per-revolution (1/rev) blade pitch variation. Figure 1 shows the principle of the special hardware fitted to the DFVLR rotor test rig which allows a precise blade root pitch control with any combination of 3/rev, 4/rev, and 5/rev frequencies. The required high frequency oscillation of the conventional swashplate is performed by computer controlled electro-hydraulic actuators. The same hardware was used to modify the blade root pitch for the attempt of reducing the noise radiation during BVI test conditions.

### 3 Test Set-up and Procedures

In Figure 2 the DFVLR rotor test stand is shown installed in the DNW 6m by 8m closed test section, which was chosen to achieve the total flight envelope of the BO-105. The 4m diameter rotor is a 40-percent, dynamically scaled model of a four-bladed, hingeless BO-105 main rotor [8]. The instrumentation layout of the experiment was primarily designed for the HHC vibration reduction tests [22]. It is self-evident that the rotor and the

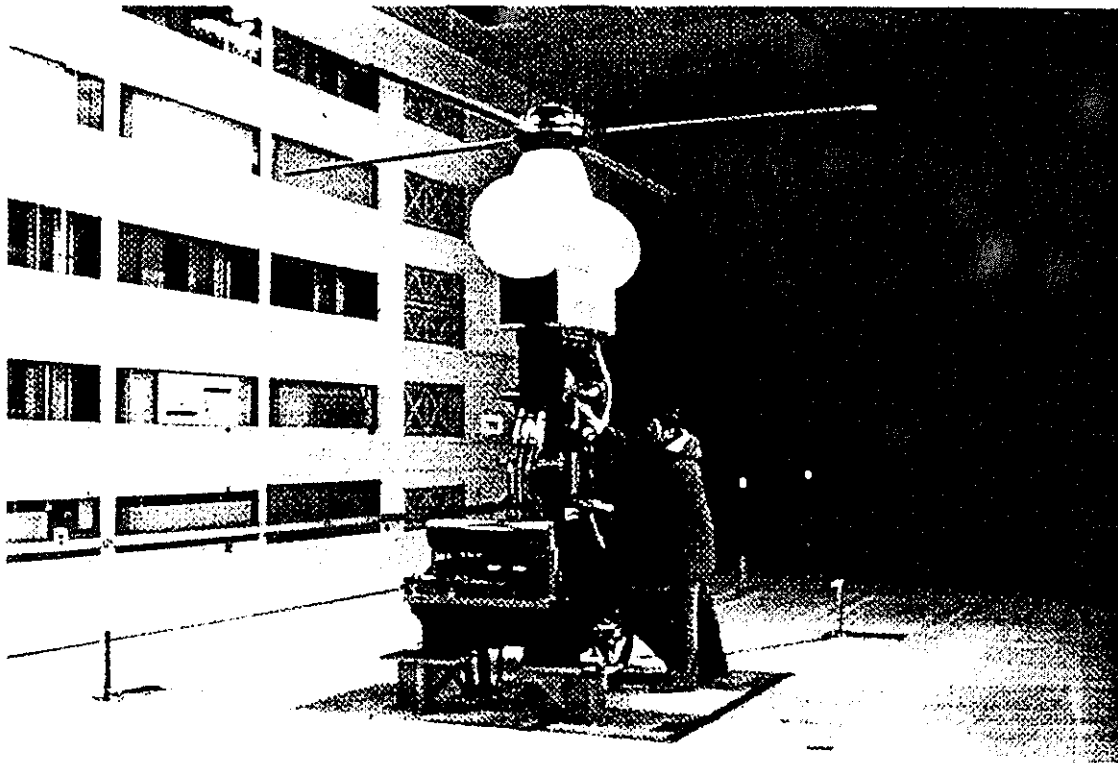


Fig. 2 Photograph of the HHC experimental apparatus (BO-105 rotor) installed in the DNW closed 6m x 8m test section

test rig was fully instrumented to monitor all important test conditions related to this test objective. The data acquisition system (PCM) acquired roughly 48 samples per rotor revolution from each of the 64 sensors so that data analysis in the frequency domain can be performed up to the 9-th rotor harmonic. Samples of all measurements from each test point were stored on digital tape. In parallel (as back-up) all PCM data were continuously recorded on a special video system with a storage capacity of 2.4 GBytes per cassette.

In the case of minimizing the vibration level by HHC the computer system calculates online a quality criterion (GF) which is based on the 4/rev components (X,Y,Z force components; L,M moments) of the rotor balance:

$$GF = (X^2 + Y^2 + Z^2 + L^2 + M^2)^{1/2}$$

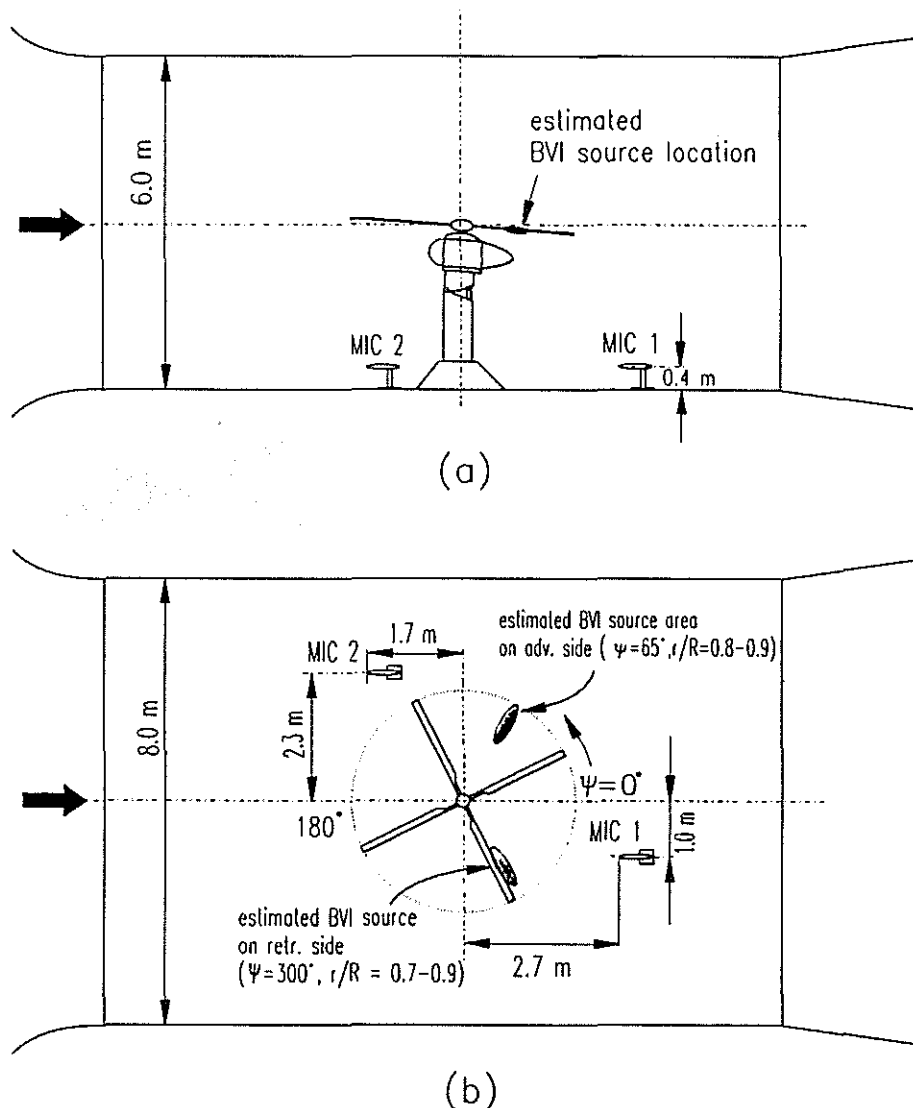


Fig. 3 Diagram of the test set-up in the DNW closed test section illustrating microphone installation; (a) side view, (b) top view

This GF function has a minimum at the lowest vibration level. The value of GF was continuously displayed so that the operator could observe the variation and was able to adjust the HHC inputs correctly. In order to obtain comparable results to the BO-105 full-scale rotor, the model rotor was operated to match the four nondimensional parameters: thrust coefficient  $C_T$ , hover tip Mach number  $M_H$ , advance ratio  $\mu$ , and rotor tip path plane angle  $\alpha_{TPP}$ . This was accomplished in the following manner: At first, the collective pitch was chosen from BO-105 flight test data, then the shaft tilt angle was adjusted until the rotor had the scaled thrust or equivalent the identical thrust coefficient ( $C_T = 0.0044$ ), and finally the rotor moments were trimmed to zero using the cyclic pitch control.

The additional higher harmonic pitch control was applied as follows: One of the three HHC modes (e.g. 3/rev.) and the amplitude of the blade pitch angle (e.g. 0.4 degrees) was selected and properly adjusted. Then the phase of the higher harmonic pitch angle was shifted from 0 to 360 degrees in increments of 30 degrees at most. At each control phase setting the data acquisition was started for a few seconds duration and a data point was taken.

For the acoustic measurements two 1/4-inch condenser microphones were installed in the closed test section, one under the advancing side and the other one under the retreating side of the rotor, as shown in Fig. 3 (also visible in the photograph of Fig. 2). The microphones were placed at locations known from previous tests [8, 9] to receive strong BVI impulsive noise radiation at typical low speed BVI test conditions.

The acoustic data acquisition- and analysis-system is shown in Fig. 4. After proper calibration and amplification the microphone signals were stored on a two-channel analogue tape recorder for off-line analysis, and - as back-up - on the two voice-tracks of the PCM video system. Narrow band spectra (0 - 1.6 kHz), 1/3-octave-spectra (upper boundary 20 kHz) as well as A-weighted noise levels were generated off-line, and used to demonstrate the HHC effect on the BVI noise radiation.

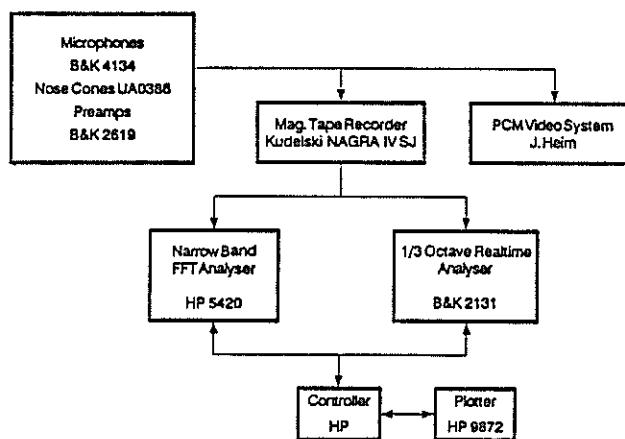


Fig. 4 Acoustic data acquisition and analysis system

Some care must be taken, when interpreting the acoustic measurement results. One important restriction might be imposed due to the fixed microphone position. A possible change in noise radiation directivity when HHC is active, would only be measured with a moving microphone rig. Another point is that the acoustic signals possibly are contaminated by sound reflections off the hard walls of the acoustically untreated test section and test hardware.

However, it is thought that due to the well known excellent flow quality of the DNW and the low turbulence and background noise levels, and due to the relative measurement method at fixed positions without and with HHC activated, acceptable results were obtained. In Fig. 5 a narrow band

spectrum of the rotor noise for a typical BVI condition measured under the advancing side is compared to the tunnel background noise, showing an excellent signal-to-noise ratio. The results therefore, will allow at least a qualitative evaluation of the HHC effect on the BVI impulsive noise generation.

#### 4 Test Results

The effect of higher harmonic control on BVI noise radiation upstream and down under the advancing side of the rotor plane (measured at microphone no. 2) is shown in Fig. 6 (a) and (b) for two low speed descending flight conditions at advance ratios of  $\mu = 0.138$  and  $\mu = 0.161$ , respectively. The measured A-weighted noise levels are plotted vs. the HHC control phase for three

different modes of HHC, namely 3/rev, 4/rev and 5/rev control modes and 0.4 degrees pitch angle amplitude. For each case the magnitude of noise reduction, but also of excess noise generation can be easily assessed versus the basic case noise radiation measured without HHC active (also plotted in the diagrams). For both operating conditions considerable noise reductions of more than 4 dB(A) is measured for certain control phase angles being different for each of the control modes (this is equivalent to more than 40% reduction of the acoustic pressure). For the strong BVI operating condition ( $\mu = 0.138$ ) the optimum noise reduction was obtained for the 4/rev HHC mode at a control phase angle near 120 degrees. For the  $\mu = 0.161$  condition the optimum noise reduction was performed for the 3/rev mode at a control phase angle near 30 degrees. The other HHC control modes also yield considerable noise reductions. The reason for the actual BVI noise reduction - explained later in detail - is, that the effective angle of attack and thus the actual blade loading is being reduced while simultaneously the blade vortex miss-distance is increased in the first quadrant between 45 and 90 degrees azimuth at the outer span, where strong blade-vortex interactions occur.

Fig. 6 however, also indicates that for certain other combinations of HHC mode and control phase angles an increase of BVI noise radiation (in the order of 3 dB(A)) was measured, and it was found that these control settings are in the range of optimum vibration control. These initial results indicate that optimum noise control likely is accompanied by increased vibration levels and vice versa.

The effects of HHC on BVI noise generation can be studied in more detail, when the noise spectra for different HHC control settings are compared. For this comparison the strong BVI rotor operating condition at  $\mu=0.161$ ,  $\alpha_{TPP} = 1.8^\circ$  and the 3/rev HHC mode with  $0.4^\circ$  pitch angle amplitude

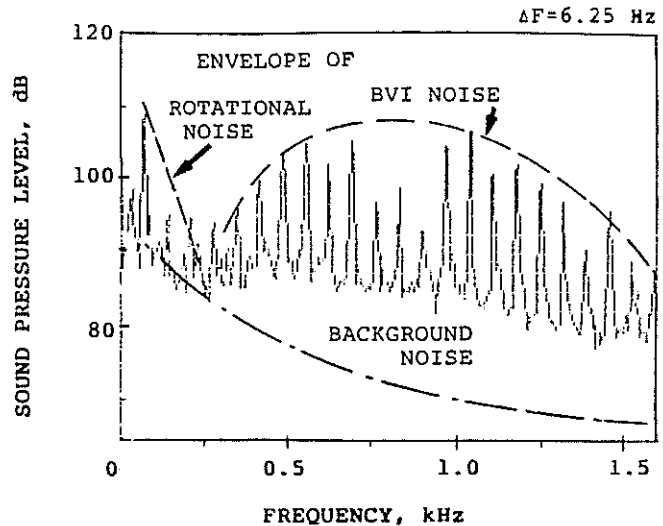


Fig. 5 Rotor noise without HHC compared to tunnel background noise under advancing side at microphone 2 (rotor condition:  $\mu=.161$ ,  $\alpha_{TPP}=1.8^\circ$ ,  $M_H=.64$ ,  $C_T=.0044$ )

for two significant control phase angles have been selected. In Fig. 7 the one-third-octave spectra for optimum noise reduction control phase angle of  $30^\circ$  (Fig. 7(a)) and for optimum vibration reduction control phase angle of  $180^\circ$  (Fig. 7(b)) are plotted together with the basic spectrum without HHC active for easy comparison. The optimum noise control clearly shows a noise level reduction in the frequency range above 300 Hz typical for BVI noise radiation, while the diagram below for optimum vibration control indicates the excess noise generation for most of the BVI frequency bands.

The large amplitude signal at the lower frequency 80 Hz band represents the blade passage frequency harmonic of the rotor rotational noise, which appears also affected by HHC, particularly for optimum BVI noise control setting (Fig. 7a) showing considerable excess noise. This unwanted effect was not found for another test case and should be further persued.

The beneficial effect of HHC on BVI noise at optimum noise control and the opposite effect at optimum vibration control is still more obvious in Fig. 8 (a) and (b), respectively where the narrow band spectra (band width 6.25 Hz) are plotted for both cases. The operational test conditions, the HHC mode and phase angles are the same as for Fig. 7. For ease of comparison the envelope of the harmonics of the rotational and the BVI impulsive noise of the basic test case without HHC active (see Fig. 5) are included in each of the diagrams.

Although the spectral levels might be affected by reflections off the hard tunnel walls, the trend of these relative measurements at the identical location known to receive maximum BVI noise radiation, appears to be clear: At a particular control phase angle (here  $30^\circ$ ) optimum noise reduction can be achieved (Fig. 8(a)) with considerably reduced levels of BVI impulsive noise, while at a particular however different phase angle (here  $180^\circ$ ) optimum vibration reduction is obtained with increased levels of the BVI frequency content and vice versa as stated above.

Similar trends were observed for retreating side BVI simultaneously

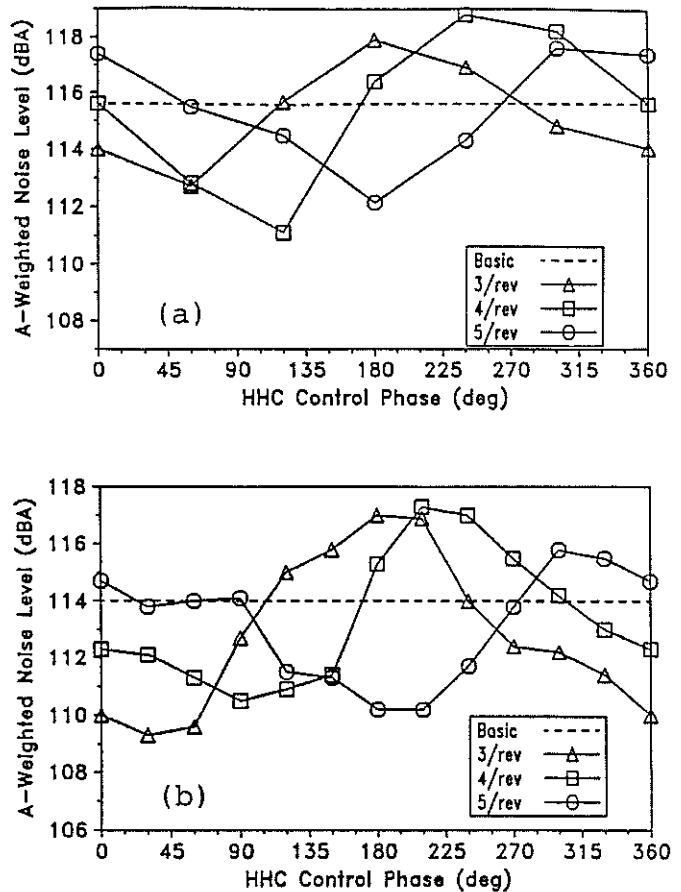


Fig. 6 HHC effect on BVI noise generation for different control modes and for two rotor test conditions at constant  $M_H = .64$ ;  $C_T = .0044$ ;  
(a)  $\mu = .138$ ,  $\alpha_{TPP} = 4.6^\circ$ ; (b)  $\mu = .161$ ,  $\alpha_{TPP} = 1.8^\circ$

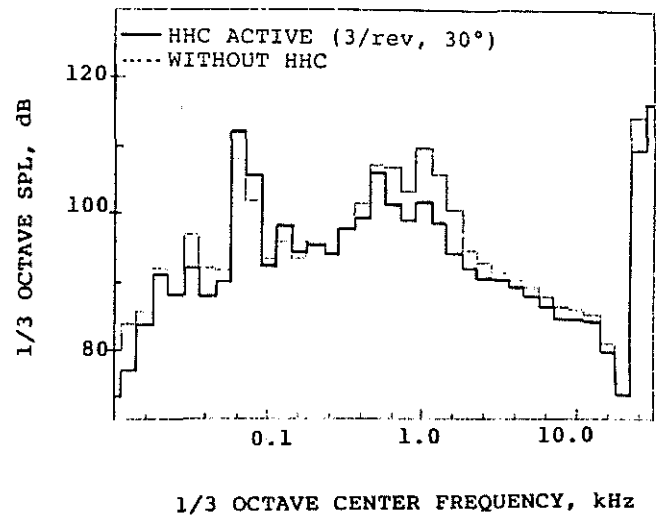
measured downstream under the retreating side (at mic.1) as is illustrated in Fig. 9 (a) and (b), although the acoustic signals are largely contaminated by additional background noise due to the close proximity of microphone 1 to the test stand support structure.

## 5 Discussion

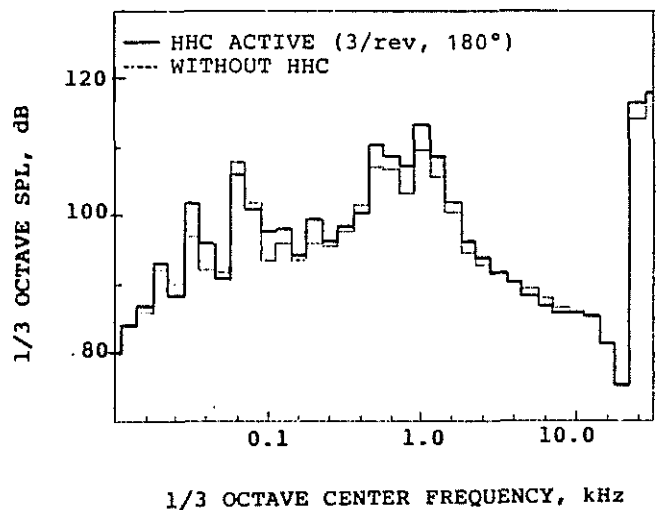
At the first glance the apparently contradictory results for noise and vibration reduction via HHC are surprising, since both effects are caused by unsteady airloads due to strong BVI in the first and fourth quadrant of the rotor plane. Initially it was thought (or hoped) that the higher harmonic control of the local blade angle of attack at any radial and azimuthal station would help to reduce these unsteady effects and thus to reduce noise and vibration at the same or at least similar control settings.

It should be noted that HHC modes of 3-, 4- and 5-per-revolution are not capable to counteract individual BVIs, which occur within a very short time period of less than one millisecond (corresponding to approx. 5 degrees azimuth), and would require a high frequency HHC mode of approximately 30/rev. Such high frequency modes however appear not feasible.

The HHC control mode of 3/rev under consideration would affect a blade azimuth angle range of 120 degrees (full period), thereby increasing or decreasing the local angle of attack over a range of 60 degrees (half period). This basic effect of HHC is illustrated in Fig. 10, where the measured blade root pitch angle (harmonic part only) is plotted vs. rotor azimuth angle. The blade pitch time histories for the significant control phase angles for optimum noise reduction (at 30°) and optimum vibration reduction (at 180°) are being compared with the basic case without HHC active.



(a)

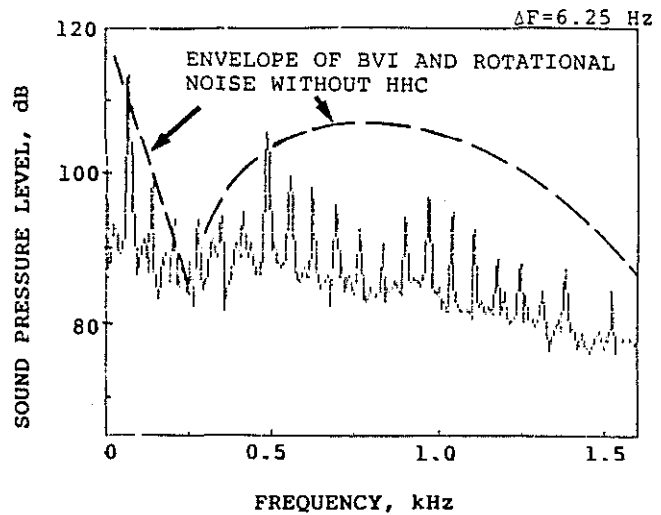


(b)

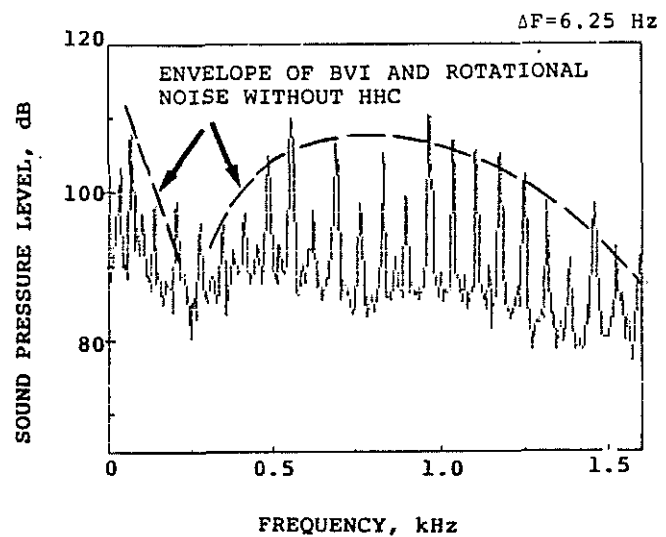
Fig. 7 HHC effect on 1/3-octave noise spectra measured under advancing side. (3/rev HHC; 0.4° pitch angle amplitude; rotor condition:  $\mu=.161$ ,  $\alpha_{TPP}=1.8^\circ$ ,  $C_T=.0044$ ,  $M_H=.64$ ); (a) Optimum BVI noise reduction control phase angle of 30°; (b) Optimum vibration reduction control phase angle of 180°

Expectedly, the optimum control settings for both, noise and vibration reduction are changing the blade root pitch angle in the first and fourth rotor plane quadrant over the blade azimuth range where strong (nearly parallel) BVIs occur, e.g. between 40 and 95, and between 270 and 330 degrees azimuth, respectively. These BVI interaction regions are illustrated in Fig. 11 (taken from [12]), where the individual BVI noise source locations as obtained via acoustic triangulation, are compared with tip vortex trajectory predictions for a rotor test condition of similar advance ratio. On close inspection of Fig. 10 it becomes quite obvious that the blade root pitch angle is decreased for optimum noise control compared to the basic case without HHC (see shaded areas in Fig. 10), while it is increased for optimum vibration control. Thus, deloading of the rotor blade in the azimuthal ranges of strong BVIs is one explanation for the BVI noise reduction potential of HHC. This is in accordance with theoretical considerations [23, 24]. Reduction of the vibratory forces is explained by the opposite effect of increasing the blade loading over the same azimuthal range of strong BVIs with the objective to prevent or at least attenuate the lift break down caused by strong (close to parallel) blade-vortex interactions in that range.

The effective deloading and the increased blade loading in the first and fourth quadrant at optimum noise and vibration control, respectively, is illustrated in Fig. 12, where the effective blade angle of attack (Fig. 12(a)), the blade loading (Fig. 12(b)) at 92% radius and the blade tip deflection (Fig. 12(c)) as obtained from rotor simulation calculations are plotted vs. blade azimuth angle.



(a)



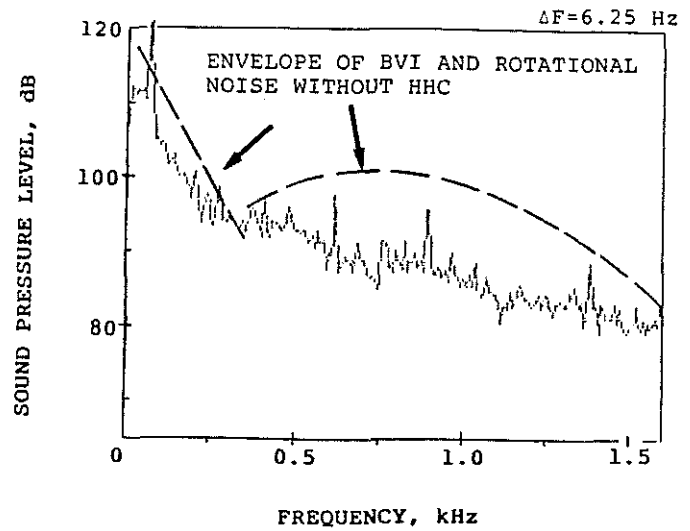
(b)

Fig. 8 HHC effect on narrow band spectra measured under advancing side (3/rev HHC: 0.4°; rotor condition as for Fig. 7); (a) Optimum BVI noise reduction control phase angle of 30°; (b) Optimum vibration reduction control phase angle of 180°

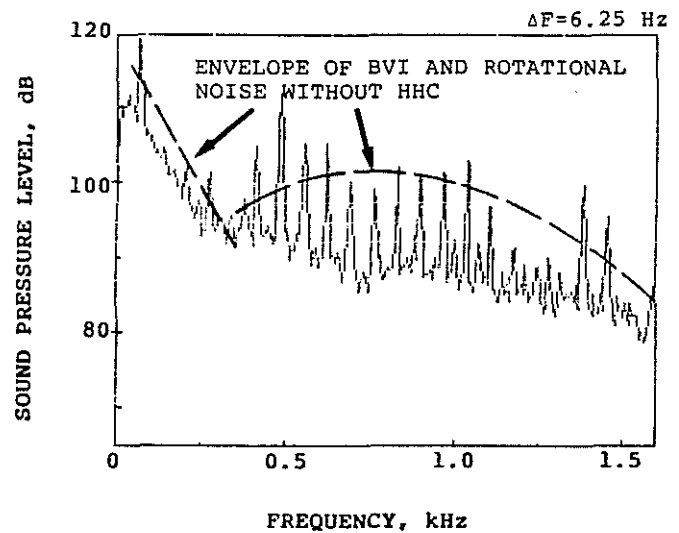
The rotor simulation calculations are based on the combination of a high resolution wake code [27] on the one hand and on a modal description of the blade elastic modes on the other, including three flapwise bending modes, two chordwise bending modes and one torsional mode. Mode shapes and eigenfrequencies are identified by a finite-element-method \*). Aerodynamic coefficients are formulated by analytical functions that are described in [28]; the parameters of this model are identified by measurements using a least-square method \*\*). This combination of high resolution codes for the wake and for blade dynamic response and also for aerodynamic coefficients yields very good predictions of vibrational forces and moments of the rotor. The calculated quality criterion for both, the basic trimmed condition and the case of higher harmonic input agrees well with measurements, so that the calculated effects near the blade tip seem to be very reliable.

The results shown in Fig. 12 were obtained for a trimmed condition\*\*) with zero moment about the rotor longitudinal and lateral axis and at operating conditions of  $\mu = 0.161$ ,  $\alpha_{TPP} = 1.8^\circ$ ,  $M_H = 0.64$  and  $C_T = 0.0044$ .

Possible contributions of the alternate basic BVI noise generating parameters (vortex strength and blade-vortex separation distance) to the measured noise reduction can be studied by more detailed inspection of the blade loading and tip deflection time-histories of Fig. 12 (b) and (c), respectively. HHC for optimum noise reduction yields an increase in tip deflection at the blade azimuth ranges of advancing and retreating side BVI (see Fig 12 (c), shaded areas) and simultaneously a tip deflection decrease



(a)



(b)

Fig. 9 HHC effect on narrow band spectra measured under retreating side (3/rev HHC:  $0.4^\circ$ ; rotor condition as for Fig. 7); (a) Optimum BVI noise reduction control phase angle of  $30^\circ$ ; (b) Optimum vibration reduction control phase angle of  $180^\circ$

\*) DFVLR IB 154-80/21

\*\*) DFVLR IB 111-87/38

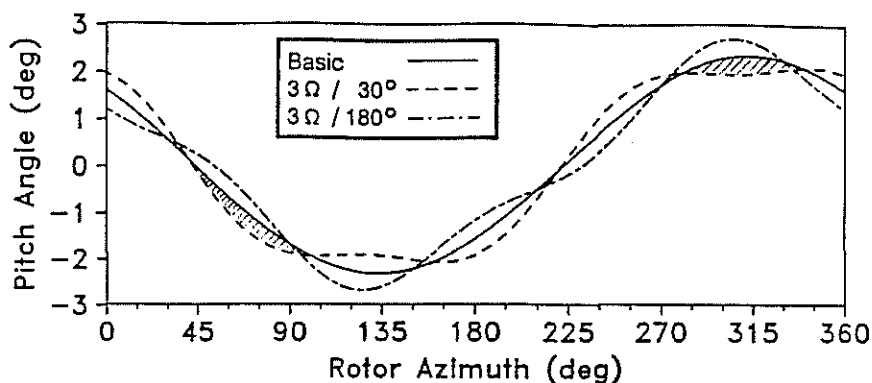


Fig. 10 Measured blade root cyclic pitch angle vs. rotor azimuth angle with 3/rev HHC control settings for BVI noise reduction (30° phase shift) and vibration reduction (180° phase shift) compared to basic case without HHC

at the blade azimuthal ranges, where the interacting tip vortices are being generated (see pointers in Fig. 12 (c)). In total, a considerable increase in blade vortex miss-distance (in the order of 10% blade chord or equivalent in the order of the vortex core-size) is calculated. Since the blade vortex separation- (or miss-) distance is inversely squared proportional to BVI noise generation, this alternate HHC effect might represent the most important parameter however, this has to be proved by additional measurements.

This beneficial effect of HHC will be partly offset by the simultaneous increase in vortex strength, indicated by increased blade loading over the blade azimuthal ranges where the interacting vortices are being generated (see pointers in Fig. 12(b)).

HHC control settings for optimum vibration reduction, unfortunately, show adverse effects on all of the three basic BVI noise generating parameters (see Fig. 12) with the resulting effect of BVI noise increase.

The highly interesting however more qualitative results of this initial experiment should be validated by future testing with improved acoustic measurement equipment in an anechoic environment.

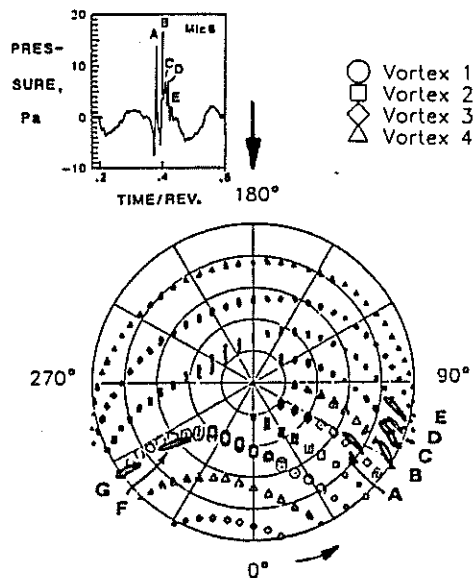


Fig. 11 BVI source locations compared with wake predictions [12], rotor condition:  $\mu=.15$ ,  $\alpha_{Tpp}=-1.4^\circ$ ,  $C_T=.0044$ ,  $M_H=.64$  (Insert: related BVI impulsive noise time-history)

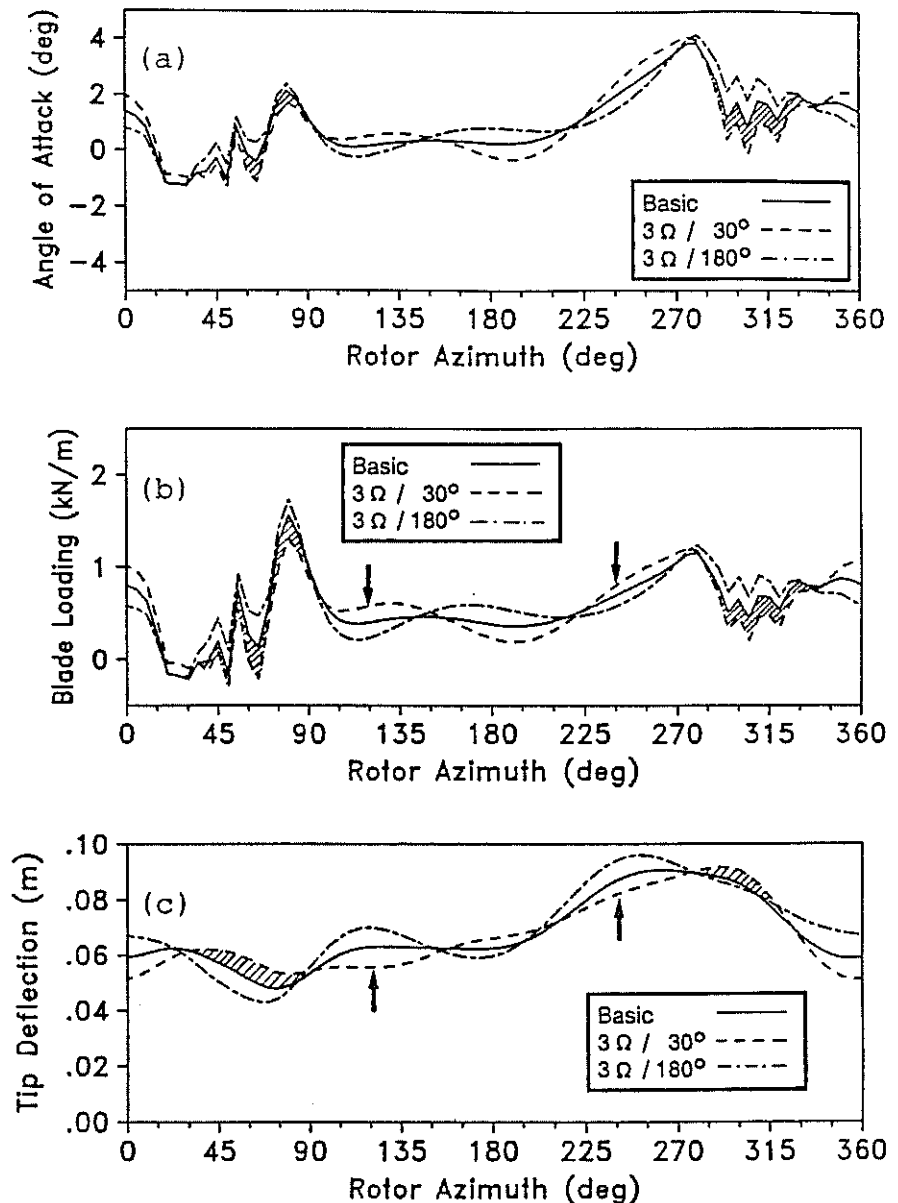


Fig. 12 Rotor simulation results at 92% blade radius vs. rotor azimuth with/without HHC active (parameters as for Fig. 7); (a) Effective blade angle of attack; (b) Blade loading; (c) Blade tip deflection

## 6 Conclusions

The initial higher harmonic control (HHC) wind tunnel experiment on blade-vortex interaction (BVI) impulsive noise reduction has at least qualitatively demonstrated that BVI noise generation can considerably be influenced by the choice of HHC mode and control phase.

Preliminary results indicate that all of the three basic parameters of BVI noise generation appear to be affected by HHC. At optimum control settings for BVI noise reduction the blade loading is decreased, the vortex strength and the blade vortex miss-distance are increased over the azimuthal ranges of nearly parallel BVI in the first and fourth quadrant. A considerable noise reduction was achieved (in the order of 4 to 5 dB(A)).

At optimum HHC control settings for vibration reduction adverse effects on blade loading, vortex strength and blade vortex miss-distance are

observed, resulting in increased BVI noise generation (in the order of 3 dB(A)).

The adverse HHC effects of significantly reduced BVI noise levels at the cost of increased vibration levels and vice versa as well as some restrictions imposed on the acoustic data quality, require further investigations into validation and optimization of the HHC potential for noise and vibration reduction.

### References

1. Schmitz, F.H. and Boxwell, D.A.: In-Flight Far-Field Measurement of Helicopter Impulsive Noise. Preprint No. 1062, Proc. 33rd Annual National V/STOL Forum of the American Helicopter Soc., 1976.
2. Boxwell, D.A. and Schmitz, F.H.: Full-Scale Measurements of Blade Vortex Interaction Noise. Preprint No. 8061, Proc. 36th Annual Forum, American Helicopter Soc., 1980.
3. Charles, B.D.: Acoustic Effects of Rotor-Wake Interaction During Low Power Descent. Proc. of National Symposium on Helicopter, Aerodynamic Efficiency, American Helicopter Soc., 1975, pp. 7.1-7.8.
4. Cox, C.R.: Helicopter Rotor Aerodynamic and Aeroacoustic Environments. AIAA 77-1338, Oct. 1977.
5. Schlinker, R.H., and Amiet, R.K.: Rotor-Vortex Interaction Noise. NASA CR 3744, Oct. 1983.
6. Splettstoesser, W.R., Schultz, K.-J., Boxwell, D.A., and Schmitz, F.H.: Helicopter Model Rotor-Blade Vortex Interaction Impulsive Noise: Scalability and Parametric Variations. NASA TM 86007, December 1984.
7. Leighton, K.P., and Harris, W.L.: On Mach Number Scaling of Blade/Vortex Noise Produced by Model Helicopter Rotors at Moderate Tip Speeds. FDRL Report 84-3, Massachusetts Inst. of Technology, Oct. 1984.
8. Martin, R.M., and Splettstoesser, W.R.: Acoustic Results of the Blade-Vortex Interaction Test of a 40 Percent Model Rotor in the DNW. Proc. of the AHS Specialist's Meeting on Aerodynamics and Aeroacoustics, Arlington, Texas, Feb. 1987.
9. Martin, R.M., Splettstoesser, W.R., Elliott, J.W., and Schultz, K.-J.: Advancing Side Directivity and Retreating Side Interactions of Model Rotor Blade-Vortex Interaction Noise. NASA TP 2784, AVSCOM TR 87-B3, May 1988
10. Martin, R.M., Elliott, J.W., Hoad, D.R.: Comparison of Experimental and Analytical Predictions of Rotor Blade-Vortex Interactions Using Model Scale Acoustic Data. AIAA-84-2269, Oct. 1984.
11. Hoad, D.R.: Helicopter Blade-Vortex Interaction Locations - Scale-Model Acoustics and Free-Wake Analysis Results. NASA TP 2658, April 1987.
12. Splettstoesser, W.R., Schultz, K.-J., Martin, R.M.: Rotor Blade-Vortex Interaction Impulsive Noise Source Identification and Correlation with Wake Predictions. AIAA-87-2744, Oct. 1987.

13. Ffowcs Williams, J.E. and Hawkings, D.L.: Sound Generated by Turbulence and Surfaces in Arbitrary Motion, Philos. Trans. R.Soc London, Ser.A, Vol. 264, May 1969, pp. 321-342.
14. Farassat, F., Theory of Noise Generation from Moving Bodies with an Application to Helicopter Rotors, NASA TR R-451, Dec. 1975.
15. Schmitz, F.H. and Yu, Y.H.: Helicopter Impulsive Noise: Theoretical and Experimental Status, NASA TM 84390, Nov. 1983.
16. Nakamura, Y., Prediction of Blade-vortex Interaction Noise from Measured Blade Pressure, Paper No. 32, Proc. 7th European Rotorcraft and Powered Lift Aircraft Forum, Garmisch-Partenkirchen, Federal Republic of Germany, 1981.
17. Schultz, K.-J. and Spletstoeser, W.R.: Measured and Predicted Impulsive Noise Directivity Characteristics, Paper No. 1.2, Proc. 13th European Rotorcraft Forum, Paper No. 1.2, Arles, France, Sep. 1987.
18. Joshi, M.C., Lin, S.R., Boxwell, D.A.: Prediction of Blade-Vortex Interaction Noise. Proc. 43rd Annual Forum, American Helicopter Soc., May 1987, pp. 405-420.
19. Brentner, K.S.: A Prediction of Helicopter Rotor Discrete Frequency Noise for Three Scale Models Using a New Acoustics Program, AIAA 25th Aerospace Science Meeting, Reno, Nevada, 1987.
20. Lehmann, G.: The Effect of HHC to a Four Bladed Hingeless Model Rotor. Paper No. 64, Proc. Tenth European Rotorcraft Forum, The Hague, The Netherlands, Aug. 1984.
21. Lehmann, G.: Untersuchungen zur höherharmonischen Rotorblattsteuerung bei Hubschraubern. DFVLR-FB 87-36, 1987.
22. Lehmann, G., Kube, R.: Automatic Vibration Reduction at a Four Bladed Hingeless Model Rotor - A wind Tunnel Demonstration. Paper No. 60, Proc. Fourteenth European Rotorcraft Forum, Milano, Italy, Sept. 1988.
23. Hardin, J.C., Lamkin, S.L.: Concepts for Reduction of Blade-Vortex Interaction Noise. AIAA-86-1855, July 1986.
24. George, A.R. and Chang, S.B.: Noise Due to Blade-Vortex Interactions. Paper No. A-83-39, Proc. 39th Annual Forum, American Helicopter Soc., 1983.
25. Hoad, D.R.: Evaluation of Helicopter Noise Due to Blade-Vortex Interaction for Five Tip Configurations. NASA TP 1608, Dec. 1979.
26. Spencer, R.J., Sternfeld, Jr.H., McCormick, B.W.: Tip Vortex Core Thickening for Application to Helicopter Rotor Noise Reduction. USAAVLABS TR 66-1, Fort Eustis, Virginia, Sept. 1966,
27. Beddoes, T.S., A Wake Model for High Resolution Airloads, International Conference on Rotorcraft Basic Research, Research Triangle Park, NC USA, 1985
28. Leiss, U., Wagner, S., Toward a Unified Representation of Rotor Blade Airloads with Emphasis on Unsteady and Viscous Effects, Proc. 13th European Rotorcraft Forum, Arles, 1987.